

Nonreciprocal Equilibrium 4π -Periodic Josephson Effect from Poor Man's Majorana Zero Modes

Panagiotis Kotetes,^{1,*} Mercè Roig,² and Brian M. Andersen²

¹*CAS Key Laboratory of Theoretical Physics, Institute of Theoretical Physics, Chinese Academy of Sciences, Beijing 100190, China*

²*Niels Bohr Institute, University of Copenhagen, DK-2100 Copenhagen, Denmark*

We show that the Josephson diode effect becomes possible when two coupled antiferromagnetic dimers of point-like magnetic adatoms are deposited on top of a Rashba superconductor. The degree of nonreciprocity is substantial when the arising Yu-Shiba-Rusinov (YSR) bound states approach zero energy. In this limit, these states behave as weakly coupled poor man's Majorana (PMM) excitations. The emergence of PMMs leads to highly dispersive and phase-bias asymmetric Andreev bound state dispersions. In turn, these result in a nonreciprocal Josephson current, whose diode efficiency can be controlled by varying the geometric details of the adatom's spatial configuration. In addition, thanks to spin-triplet pairing terms mixing different YSR states, the resulting Josephson effect is 4π -periodic even under equilibrium conditions. Our work opens the door to observing and harnessing Majorana behavior in currently experimentally accessible topologically trivial systems.

Introduction - Recent experiments [1–18] have unveiled a new promising functionality of Rashba spin-orbit interaction (SOI). This is, to mediate the superconducting diode effect [19–43], which manifests itself in a polarity-dependent critical supercurrent [44–47]. For the diode effect to take place, time-reversal symmetry (TRS) is also required to be violated. In the early diode experiments TRS was broken by means of an in-plane magnetic field [1, 6]. Since then, a plethora of alternative routes to realize superconducting diodes have been proposed. Amongst these, one possibility is to couple the superconductor (SC) to a spatially-nonuniform magnetization [40]. In contrast to the uniform magnetic field, tailoring the spatial profile of the magnetization allows us to control the current distribution in space and provides more knobs for optimizing the diode efficiency. Our previous work discusses two different scenarios, i.e., a uniform gradient and a ferromagnetic domain wall [40]. In either case, the diode effect exclusively stems from bulk electrons, and follows from the analysis of Ref. 48.

Here, we explore the superconducting diode effect which arises from magnetization gradients that are instead generated from point-like adatoms embedded in a two-dimensional Rashba SC whose phase field possesses a spatially varying profile. In Fig. 1(a) we depict the minimal setup which relies on coupled pairs of antiferromagnetic (AFM) adatoms and can lead to a superconducting diode effect. This consists of two coupled AFM adatom dimers, with their magnetic moments pointing out of the plane. Despite the fact that also here the diode effect stems from the out-of-plane magnetization gradient, the mechanisms underlying the two categories of phenomena radically differ. In the present case, the nonreciprocity of the Josephson current results solely from the Yu-Shiba-Rusinov (YSR) states [49] induced by the adatoms.

Our analysis reveals that the diode effect becomes substantial when the energy of the YSR states is near zero. In fact, the combination of spin-singlet pairing and

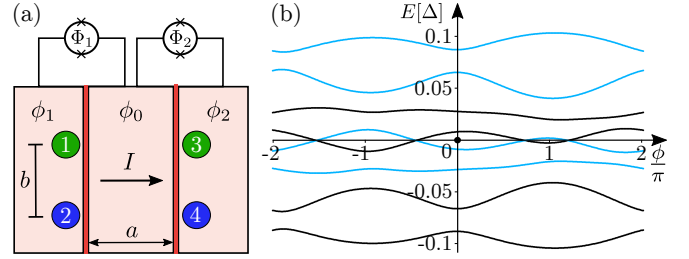


FIG. 1. (a) Sketch of the proposed setup. Two AFM adatom dimers are deposited on top of two segments of a Rashba SC which are kept at a phase difference $\phi = \phi_1 - \phi_2$, with $\phi_1 = \phi_0 - \Phi_1$ and $\phi_2 = \phi_0 + \Phi_2$, with $\Phi_{1,2}$ denoting flux biases expressed in units of phase. Here, ϕ_0 is the phase of the middle Rashba SC. The spin moments of the “1,3” (“2,4”) adatoms are pointing out of (in to) the page. (b) Typical YSR band structure obtained for (a). The dispersions are 4π -periodic and realize the Josephson diode effect even in equilibrium.

Rashba SOI ensures that the zero YSR states behave similar to Majorana zero modes (MZMs), albeit that they have a fine-tuned rather than a topological origin [50–53]. Nonetheless, we show that these so-called poor man's Majoranas (PMMs) endow the Josephson current with characteristics that are typical to MZMs [54–72]. Specifically, we find that the current $I(\phi)$ can be both nonreciprocal and 4π -periodic in terms of the phase bias $\phi = \phi_1 - \phi_2$, with $\phi_{1,2}$ the phases felt by the two dimers. Notably, the 4π -periodicity arises even in equilibrium, due to the phase ϕ_0 of the middle SC in Fig. 1(a) [59, 61, 66–70]. After prior findings for MZMs [59, 61], such junctions simultaneously take two energy contributions, i.e., $\propto \cos[(\phi_1 - \phi_2)/2]$ and $\propto \cos[(\phi_1 + \phi_2)/2 - \phi_0]$. These two combined generally render the current 4π -periodic. In the remainder, we explore the Josephson current upon varying the intra-dimer distance and the exchange coupling strength between electrons and magnetic moments.

Modeling the system - The Rashba SC is described using the continuum Bogoliubov - de Gennes (BdG) Hamiltonian:

$$\hat{H}_0(\mathbf{p}) = \tau_z [\varepsilon(p) + v(p_x \sigma_y - p_y \sigma_x)] + \Delta \tau_x, \quad (1)$$

where \mathbf{p} is the momentum, $\sigma_{x,y,z}$ denote the spin Pauli matrices, $v \geq 0$ is the Rashba SOI strength, and $\Delta \geq 0$ defines the spin-singlet pairing gap. In addition, we employ the energy dispersion $\varepsilon(p) = (p^2 - p_F^2)/2m_*$, with m_* the effective mass, p_F the Fermi momentum of the system for $v = \Delta = 0$, and $p = |\mathbf{p}|$. The above ‘‘single’’-particle Hamiltonian is expressed in the Nambu space spanned by electrons with spin up and down, along with their hole partners after acting on them with the time-reversal operator $\hat{T} = i\sigma_y \hat{K}$, where \hat{K} effects complex conjugation. Operators in Nambu space are represented with the help of the Pauli matrices $\tau_{x,y,z}$. For convenience of notation, the respective unit matrices in spin, Nambu, and other spaces are omitted throughout, and we set $\hbar = 1$ for the reduced Planck constant.

We now proceed with the adatoms. These are assumed to have a spatial extent which is smaller than the Fermi wavelength $\lambda_F = 2\pi/p_F$. For this reason, we model them as point-like objects. Moreover, their magnetic moments are considered classical and oriented out of the system’s plane. In their presence, the coordinate space BdG Hamiltonian takes the additional contribution $\hat{V}(\mathbf{r}) = \sum_n \hat{V}_n \delta(\mathbf{r} - \mathbf{R}_n)$, where \mathbf{R}_n are the positions of the adatoms in coordinate space. The terms $\hat{V}_n = JS_n \sigma_z$ denote the exchange interactions of electrons with the localized spins $S_n = \pm 1$, where J is the coupling strength.

Effective YSR Hamiltonian - The addition of the classical magnetic adatoms induces YSR bound states in the underlying Rashba SC [49]. The YSR energy spectrum can be obtained from the poles of the so-called T-matrix [73]. After the results of prior studies [74–78], projecting the T-matrix onto two adatom positions $\mathbf{R}_{n,m}$ and restricting to energies which are much smaller than Δ , leads to the YSR coupling Hamiltonian elements:

$$\hat{H}_{nm} = \left[\tau_x + (\pi\nu_F \hat{V}_n)^{-1} \right] \delta_{nm} + (1 - \delta_{nm}) \hat{g}_{nm}, \quad (2)$$

with the energy expressed in units of Δ . In the above, δ_{nm} is the Kronecker delta and $\nu_F = m_*/2\pi$ is the density of states per spin at the Fermi level when $v = \Delta = 0$. We also defined the off-diagonal Hamiltonian elements $\hat{g}_{nm} \equiv \hat{g}(\mathbf{R}_{nm})$, which are functions of the relative position vector $\mathbf{R}_{nm} = \mathbf{R}_n - \mathbf{R}_m \equiv R_{nm} (\cos \theta_{nm}, \sin \theta_{nm})$ with $R_{nm} = |\mathbf{R}_{nm}|$. In the remainder, we assume that $p_F R_{nm} > \pi$. In this regime, previous results [78] yield:

$$\hat{g}(\mathbf{R}) = f(R) e^{-i\zeta(R)\tau_y \tau_x} \left\{ \cos[\eta(R)] - i \sin[\eta(R)] \sigma_y e^{i\theta \sigma_z} \right\} \quad (3)$$

where we momentarily suppressed the indices n and m .

We observe the presence of three new parameters. The first is $f(R) = \text{Exp}(-R\Delta/v_F) \sqrt{2/(\pi p_F R)}$, with the Fermi velocity $v_F = p_F/m_*$, and controls the overall strength of the YSR coupling. Next, is the variable $\eta(R) = m_* v R$ which results from the Rashba SOI and controls the ratio between spin-singlet and triplet hopping terms. Lastly, the parameter $\zeta(R) = p_F R - \pi/4$ tunes the ratio between electron and pair hoppings, which enter in the Hamiltonian with terms $\propto \tau_z$ and $\propto \tau_x$, respectively. From now on, we choose to express all length scales in units of λ_F . This allows us to write the above coefficients solely in terms of the three dimensionless quantities: $R/\lambda_F > 1/2$, $\Delta/E_F \ll 1$ and $2m_* v/p_F \ll 1$. In the remainder, we consider $\Delta/E_F = 2m_* v/p_F = 0.1$ and set $a/\lambda_F = 2.8$, for all our numerical calculations. Moreover, we neglect any suppression of the electron and pair hoppings due to the junction barriers shown in Fig. 1(a), since these can be absorbed by rescaling a , Δ , and M .

We now proceed by inferring the Hamiltonian which describes the coupled YSR states obtained in the setup of Fig. 1(a). The Hamiltonian for an isolated dimer, whose pair of adatoms are separated by a distance b , reads:

$$\hat{H}_{\text{intra}} = \tau_x + M \rho_z \sigma_z + f_b e^{i(\eta_b \rho_z \sigma_x - \zeta_b \tau_y)} \rho_x \tau_x \quad (4)$$

where the index b in the respective coefficients denotes that these are evaluated for this value of distance. The dimensionless variable $M = (\pi\nu_F J)^{-1}$ controls the strength of the exchange coupling. To express the Hamiltonian in the two-state space of adatoms which comprise a single dimer, we employ the Pauli matrices $\rho_{x,y,z}$, with $\rho_z = \pm 1$ labelling adatoms ‘‘1,3’’ and ‘‘2,4’’ in Fig. 1(a). The two dimers further couple to each other through:

$$\begin{aligned} \hat{H}_{\text{inter}} = & f_a e^{i(\eta_a \lambda_z \sigma_y - \zeta_a \tau_y)} \lambda_x \tau_x + f_c \cos(\eta_c) e^{-i\zeta_c \tau_y} \lambda_x \rho_x \tau_x \\ & - f_c \sin(\eta_c) e^{-i\zeta_c \tau_y} (\cos \theta \lambda_y \rho_x \tau_x \sigma_y + \sin \theta \lambda_x \rho_y \tau_x \sigma_x), \end{aligned} \quad (5)$$

where $\tan \theta = b/a$. Hamiltonian elements in the dimer space are expressed using the Pauli matrices $\lambda_{x,y,z}$. Here, $\lambda_z = +1$ ($\lambda_z = -1$) corresponds to the left (right) dimer.

The total YSR Hamiltonian $\hat{H}_{\text{YSR}} = \hat{H}_{\text{intra}} + \hat{H}_{\text{inter}}$ possesses a chiral symmetry effected by $\hat{\Pi} = \lambda_x \tau_y \sigma_x$, a generalized TRS symmetry effected by $\hat{\Theta} = \lambda_x \sigma_z \hat{K}$, and a charge-conjugation symmetry induced by $\hat{\Xi} = \tau_y \sigma_y \hat{K}$. The latter guarantees that zero energy eigenstates are of the PMM type. Due to their topologically trivial origin, these need to come in pairs. In the absence of additional symmetries, \hat{H}_{YSR} is in BDI symmetry class [79]. However, \hat{H}_{YSR} also features the unitary mirror symmetry effected by $\hat{\mathcal{O}} = \rho_x \sigma_y$. While this symmetry is not essential for the diode effect, its presence simplifies our presentation, as it allows us to block diagonalize \hat{H}_{YSR} . Note that this symmetry can be broken by assuming, for instance, different strengths for the exchange couplings of the electrons to the adatom moments of each dimer. Such a mismatch can be added by the term $\hat{H}_{\text{mis}} = \delta M \sigma_z$.

Up to now, all adatoms have been considered to feel the same superconducting phase. However, the Josephson effect appears only for a nonzero phase bias ϕ between the two dimers. In the remainder, we set $\phi_0 = 0$, choose $\phi_{1,2} = \pm\phi/2$, and phase twist the YSR Hamiltonian as:

$$\hat{H}_{\text{YSR}}(\phi) = \hat{H}_{\text{intra}} + e^{i\phi\lambda_z\tau_z/4}\hat{H}_{\text{inter}}e^{-i\phi\lambda_z\tau_z/4}. \quad (6)$$

Notably, the twisted Hamiltonian $\hat{H}_{\text{YSR}}(\phi)$ preserves all the symmetries of its untwisted counterpart \hat{H}_{YSR} .

Restricting to physical states - To proceed, we note that not all of the eigenstates of $\hat{H}_{\text{YSR}}(\phi)$ are physical. Indeed, we find that half of these do not lead to eigenenergies which are much smaller than unity, a condition which we postulated in order for the form of the YSR couplings in Eq. (2) to hold. Similar to Ref. 75, we also project these out from the very beginning of our analysis.

Since throughout this work the adatoms are assumed to be only weakly coupled and $M > 0$, it is straightforward to identify the physical states with the eigenstates of the intra-dimer term $\tau_x + M\rho_z\sigma_z \equiv \tau_x(1 + M\rho_z\tau_x\sigma_z)$, which has eigenvalues $\pm(1 - M)$. Specifically, for $\rho_z = \pm 1$, we correspondingly keep the $\tau_x\sigma_z = \mp 1$ eigenstates. Moreover, with an eye to the emergence of PMMs, we choose the projected basis states to simultaneously be eigenstates of $\hat{\Xi}$. The four states are written as column vectors in $\rho \otimes \tau \otimes \sigma$ space according to the following form:

$$|1\rangle = \frac{1}{2}(+i, +i, -i, +i, 0, 0, 0, 0)^\top, \quad (7)$$

$$|2\rangle = \frac{1}{2}(-1, +1, +1, +1, 0, 0, 0, 0)^\top, \quad (8)$$

$$|3\rangle = \frac{1}{2}(0, 0, 0, 0, +i, -i, +i, +i)^\top, \quad (9)$$

$$|4\rangle = \frac{1}{2}(0, 0, 0, 0, +1, +1, +1, -1)^\top, \quad (10)$$

where \top denotes matrix transposition. By virtue of the choice of the above basis, we represent matrices in this space as Kronecker products of $\rho_{x,y,z}$ and $\kappa_{x,y,z}$ Pauli matrices along with their identity matrix companions.

Straightforward calculations lead to the projected phase-twisted Hamiltonian:

$$\begin{aligned} \hat{H}'_{\text{YSR}}(\phi) &= (1 - M)\kappa_y - f_b \cos(\zeta_b) \sin(\eta_b)\rho_y \\ &- f_b \sin(\zeta_b) \cos(\eta_b)\rho_y\kappa_x + f_a \cos(\zeta_a) \cos(\eta_a)\lambda_x\kappa_y \\ &+ f_a \sin(\zeta_a)\lambda_y [\cos(\eta_a) \sin(\phi/2) - \sin(\eta_a) \cos(\phi/2)\kappa_x] \\ &+ f_c \sin(\eta_c) [\cos(\zeta_c) \cos\theta - \sin(\zeta_c) \sin\theta \sin(\phi/2)]\lambda_y\rho_y\kappa_y \\ &- f_c \sin(\eta_c) [\cos(\zeta_c) \sin\theta + \sin(\zeta_c) \cos\theta \sin(\phi/2)]\lambda_x\rho_y \\ &- f_c \cos(\eta_c) \sin(\zeta_c) \cos(\phi/2)\lambda_x\rho_y\kappa_x. \end{aligned} \quad (11)$$

The projected Hamiltonian respects all the symmetries of the original one. However, the symmetry operators now read as $\hat{\Pi}' = \lambda_x\rho_x\kappa_x$, $\hat{\Xi}' = \hat{\mathcal{K}}$, $\hat{\Theta}' = \hat{\Pi}'\hat{\mathcal{K}}$, and $\hat{\mathcal{O}}' = \rho_y$. The charge-conjugation symmetry implies that the YSR-ABS dispersions come in pairs, i.e., $\pm\varepsilon_s(\phi)$

where $s = 1, 2, 3, 4$. On top of that, the presence of mirror symmetry allows us to replace ρ_y by its two eigenvalues $\rho = \pm 1$, and obtain two block Hamiltonians $\hat{H}'_{\text{YSR};\rho=\pm 1}$ which feature opposite eigenenergies. Hence, when mirror symmetry is present, we can associate $\varepsilon_{1,2,3,4}(\phi)$ with the four dispersions of the $\hat{H}'_{\text{YSR};\rho=+1}$ block. Lastly, in the projected space, the moment mismatch enters via the term $\hat{H}'_{\text{mis}} = -\delta M\rho_z\kappa_y$. This preserves only the charge-conjugation symmetry and enlists $\hat{H}'_{\text{YSR}}(\phi)$ in class D.

PMM Josephson effect - To study the current it is preferable to transfer to Fock space by introducing creation (annihilation) operators denoted \hat{a}_s^\dagger (\hat{a}_s) for the diagonalized YSR-ABS dispersions. These satisfy standard anticommutation relations $\{\hat{a}_s, \hat{a}_{s'}^\dagger\} = \delta_{s,s'}\hat{1}$ and $\{\hat{a}_s, \hat{a}_{s'}\} = \hat{0}$. With the help of the above, we extend the YSR-BdG Hamiltonian to a many-body framework using the mapping $\hat{H}'_{\text{YSR}}(\phi) \mapsto \hat{\mathcal{H}}'_{\text{YSR}}(\phi)$, where we introduced:

$$\hat{\mathcal{H}}'_{\text{YSR}}(\phi) = \frac{1}{2} \sum_{s=1,2,3,4} \varepsilon_s(\phi) (2\hat{a}_s^\dagger\hat{a}_s - 1). \quad (12)$$

We observe that the system's energy and the Josephson current depend on the fermion parities (FPs) of the ABSs. These are given by $\mathcal{P}_s(\phi) = 2\langle\hat{a}_s^\dagger\hat{a}_s\rangle - 1$ with $s = 1, 2, 3, 4$. Each FP takes the values ± 1 when the respective ABS state is occupied/empty. The precise value of each FP crucially depends on whether the system is in equilibrium or not [57, 60, 63]. In equilibrium, the system can exchange particles with its environment. As a result, the FP of the s -th ABS at zero temperature is given as $\mathcal{P}_s(\phi) = -\text{sgn}[\varepsilon_s(\phi)]$. In contrast, when the occupancy of each ABS is fixed during the entire measurement process, one obtains a distinct nonequilibrium Josephson current for each FP configuration. In either case, the zero-temperature Josephson current is given by:

$$I(\phi) = - \sum_s \frac{d\varepsilon_s(\phi)}{d\phi} \mathcal{P}_s(\phi), \quad (13)$$

where we set the electric charge quantum e equal to unity.

The behavior of the YSR-ABS Josephson current is directly determined by the properties of the dispersions $\varepsilon_s(\phi)$. From Eq. (11) we observe that the Hamiltonian $\hat{H}'_{\text{YSR}}(\phi)$ and, in turn, the ABS dispersions and their Josephson current lack symmetry under the inversion of the phase bias $\phi \mapsto -\phi$. Such a property is a prerequisite for obtaining a nonreciprocal Josephson effect. Furthermore, we also observe that $\hat{H}'_{\text{YSR}}(\phi + 2\pi) \neq \hat{H}'_{\text{YSR}}(\phi)$ while $\hat{H}'_{\text{YSR}}(\phi + 4\pi) = \hat{H}'_{\text{YSR}}(\phi)$. Hence, as it is typical for Hamiltonians describing coupled Majorana operators, the dependence of these couplings is 4π - instead of 2π -periodic in ϕ [56]. Note, however, that the 4π -periodicity of the Hamiltonian terms does not always imply a similar periodicity for the Josephson current [57, 60, 63, 68, 69]. Thanks to the skew-symmetric structure of the Hamiltonian, such properties of the dispersions can be more

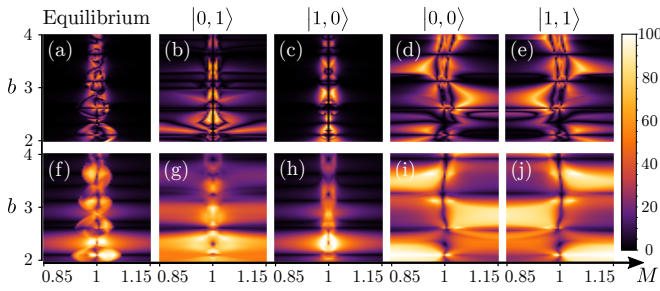


FIG. 2. Heat maps of the diode efficiency Q [%] (upper row) and the 4π -periodicity indicator P [%] (lower row), as functions of the moments strength M (in units of Δ) and the intra-dimer adatom distance b (in units of λ_F). We show results for both equilibrium and nonequilibrium cases. For the latter, we consider all four possibilities for the occupations $n_{2,3} = \{0, 1\}$ of the two middle bands $\varepsilon_{2,3}(\phi)$. Here, the energy dispersions are obtained by diagonalizing $\hat{H}'_{\text{YSR};\rho=+1}$. The nonequilibrium results are labelled according to a Fock space notation $|n_2, n_3\rangle$. The resulting bands are substantially 4π -periodic in an extended parameter regime, while the diode efficiency also reaches high values $\sim 50\%$. In fact, a high degree of 4π -periodicity is found in the even parity sector $\{|0, 0\rangle, |1, 1\rangle\}$. Moreover, the two distinct parity sectors exhibit a qualitatively different behavior, thus giving rise to for a quantum Josephson diode effect. Lastly, we observe that the equilibrium case behaves similar to the odd-parity sector.

transparently studied via the Pfaffian (Pf) of the real skew-symmetric matrix $\hat{B}(\phi) = i\hat{H}'_{\text{YSR}}(\phi)$ [56, 67, 68, 70], which satisfies the relation $\text{Pf}[\hat{B}(\phi)] = \prod_{s=1,2,3,4} \varepsilon_s(\phi)$.

Numerical results - We now proceed with the exploration of the degree of nonreciprocity and 4π -periodicity of the Josephson current. For this purpose, we introduce the two quantities (for Q see also Refs. 19, 21, and 23):

$$Q = \frac{|I_{\max}| - |I_{\min}|}{|I_{\max}| + |I_{\min}|}, P = \int_0^{2\pi} \frac{d\phi}{2\pi} \frac{|I(\phi) - I_{\text{shift}}(\phi)|}{|I(\phi)| + |I_{\text{shift}}(\phi)| + \Gamma},$$

where $I_{\max, \min}$ define the maximum and minimum values of the current $I(\phi)$, while $I_{\text{shift}}(\phi) = I(\phi + 2\pi)$. A small positive number $\Gamma = 0^+$ is added to avoid singularities when $I(\phi) = I_{\text{shift}}(\phi) = 0$. We examine equilibrium and nonequilibrium scenarios. By assuming the hierarchy $\varepsilon_1(\phi) < \varepsilon_2(\phi) < \varepsilon_3(\phi) < \varepsilon_4(\phi)$, we explore four types of nonequilibrium currents. These are obtained by fixing $\mathcal{P}_1(\phi) = +1$ and $\mathcal{P}_4(\phi) = -1$, while considering the four possible scenarios $\mathcal{P}_{2,3}(\phi) = \pm 1$ for the FPs of $\varepsilon_{2,3}(\phi)$.

Outcomes from our numerical approach are presented in Figs. 2 and 3. From the former, we confirm the non-reciprocal and 4π -periodic nature of the current. Note, however, that a strong 4π -periodicity does not necessarily imply a high diode efficiency. In Fig. 3, we show the current for two cases with an equally high diode effect $\sim 40\%$, while supporting gapless and gapped band structures. From this, we infer that band (crossings) touchings in (non)equilibrium cases tend to enhance both Q and P .

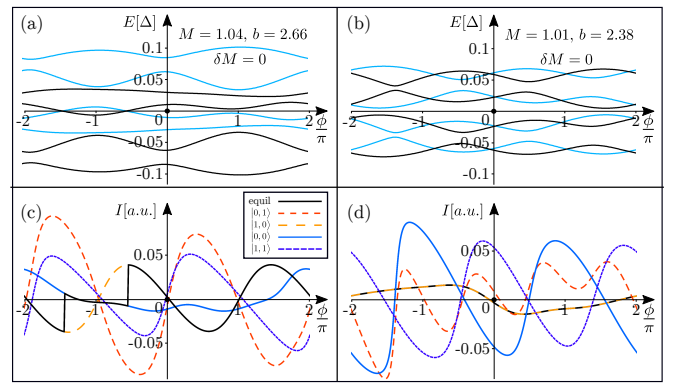


FIG. 3. Energy dispersions (a)-(b) and corresponding Josephson currents (c)-(d) for two different values for b and M . In (a) the bands contain band crossings, while in (b) there is a full gap. In (c) and (d) we show results for the equilibrium and nonequilibrium currents. For the latter, we make use of the notation introduced in Fig. 2. In (c) the maximum diode efficiency and strongest 4π -periodicity are achieved for the even-parity sector state $|0, 0\rangle$, with $Q = 40.5\%$ and $P = 80.8\%$. The corresponding values obtained for the remaining states are much smaller. (d) shows results for the odd-parity state $|0, 1\rangle$, which supports both a substantially 4π -periodic current and high diode efficiency with $Q = 37.1\%$ and $P = 67.4\%$.

Discussion - We reveal that the PMM Josephson effect is equally rich to that of MZMs. Several recent works [37–39] have discussed the impact of MZMs on the diode effect. Reference 37 examined the robustness of the effect against FP nonconservation, while the other two works restricted to equilibrium response. Here, we do not only prove that PMMs can yield a substantial diode effect with efficiencies reaching 50%, but we also show that the Josephson current is 4π -periodic even in equilibrium. Moreover, we find a quantum Josephson effect which depends on the FPs of the ABS dispersions. Notably, we expect the high efficiencies obtained here to be robust against weak disorder. For instance, we find that introducing a small moment mismatch $\delta M = 0.015$ to the case of Fig. 3(a), results to a non-substantially modified band structure, that we depict in Fig. 1(b).

Most importantly, our diode proposal is free from the requirement of topological superconductivity, which makes it promising to be realized in currently accessible platforms. First, our ideas can find applicability in already existing Majorana platforms consisting of magnetic chains embedded on Rashba SCs [80–85]. Notably, Ref. 85 already discusses AFM chains and, thus, it appears prominent for realizing the configuration in Fig. 1(a). The other possible class of systems concerns coupled quantum dots with induced superconductivity [86–91], which are purposed for engineering a Kitaev chain [92–94]. Note that Refs. 89 and 90 have already produced a PMM dimer. We hope that our work will motivate and guide diode experiments in these areas.

ACKNOWLEDGEMENTS

We are thankful to M. Cuoco, K. Flensberg, and M. T. Mercaldo for motivating and helpful discussions. M. R. acknowledges support from the Novo Nordisk Foundation grant NNF20OC0060019.

* kotetes@itp.ac.cn

- [1] F. Ando, Y. Miyasaka, T. Li, J. Ishizuka, T. Arakawa, Y. Shiota, T. Moriyama, Y. Yanase, and T. Ono, *Observation of superconducting diode effect*, *Nature* **584**, 373 (2020).
- [2] Y.-Y. Lyu, J. Jiang, Y.-L. Wang, Z.-L. Xiao, S. Dong, Q.-H. Chen, M. V. Milošević, H. Wang, R. Divan, J. E. Pearson, P. Wu, F. M. Peeters, and W.-K. Kwok, *Superconducting diode effect via conformal-mapped nanoholes*, *Nat. Commun.* **12**, 2703 (2021).
- [3] J. Díez-Mérida, A. Díez-Carlón, S. Y. Yang, Y.-M. Xie, X.-J. Gao, J. Senior, K. Watanabe, T. Taniguchi, X. Lu, A. P. Higginbotham, K. T. Law, and D. K. Efetov, *Symmetry-broken josephson junctions and superconducting diodes in magic-angle twisted bilayer graphene*, *Nat. Commun.* **14**, 2396 (2023).
- [4] J. Yun, S. Son, J. Shin, G. Park, K. Zhang, Y. J. Shin, J.-G. Park, and D. Kim, *Magnetic proximity-induced superconducting diode effect and infinite magnetoresistance in a van der Waals heterostructure*, *Phys. Rev. Res.* **5**, L022064 (2023).
- [5] J.-X. Lin, P. Siriviboon, H. D. Scammell, S. Liu, D. Rhodes, K. Watanabe, T. Taniguchi, J. Hone, M. S. Scheurer, and J. I. A. Li, *Zero-field superconducting diode effect in small-twist-angle trilayer graphene*, *Nat. Phys.* **18**, 1221 (2022).
- [6] C. Baumgartner, L. Fuchs, A. Costa, S. Reinhardt, S. Gronin, G. C. Gardner, T. Lindemann, M. J. Manfra, P. E. Faria Junior, D. Kochan, J. Fabian, N. Paradiso, and C. Strunk, *Supercurrent rectification and magnetochiral effects in symmetric Josephson junctions*, *Nat. Nanotechnol.* **17**, 39 (2022).
- [7] E. Strambini, M. Spies, N. Ligato, S. Ilić, M. Rouco, C. González-Orellana, M. Ilyn, C. Rogero, F. S. Bergeret, J. S. Moodera, P. Virtanen, T. T. Heikkilä, and F. Giazotto, *Superconducting spintronic tunnel diode*, *Nat. Commun.* **13**, 2431 (2022).
- [8] H. Wu, Y. Wang, Y. Xu, P. K. Sivakumar, C. Pasco, U. Filippozzi, S. S. P. Parkin, Y.-J. Zeng, T. McQueen, and M. N. Ali, *The field-free Josephson diode in a van der Waals heterostructure*, *Nature* **604**, 653 (2022).
- [9] L. Bauriedl, C. Bäuml, L. Fuchs, C. Baumgartner, N. Paulik, J. M. Bauer, K.-Q. Lin, J. M. Lupton, T. Taniguchi, K. Watanabe, C. Strunk, and N. Paradiso, *Supercurrent diode effect and magnetochiral anisotropy in few-layer NbSe₂*, *Nat. Commun.* **13**, 4266 (2022).
- [10] Y. Hou, F. Nichele, H. Chi, A. Lodesani, Y. Wu, M. F. Ritter, D. Z. Haxell, M. Davydova, S. Ilić, O. Glezakou-Elbert, A. Varambally, F. S. Bergeret, A. Kamra, L. Fu, P. A. Lee, and J. S. Moodera, *Ubiquitous Superconducting Diode Effect in Superconductor Thin Films*, *Phys. Rev. Lett.* **131**, 027001 (2023).
- [11] B. Pal, A. Chakraborty, P. K. Sivakumar, M. Davydova, A. K. Gopi, A. K. Pandeya, J. A. Krieger, Y. Zhang, M. Date, S. Ju, N. Yuan, N. B. M. Schröter, L. Fu, and S. S. P. Parkin, *Josephson diode effect from Cooper pair momentum in a topological semimetal*, *Nat. Phys.* **18**, 1228 (2022).
- [12] B. Turini, S. Salimian, M. Carrega, A. Iorio, E. Strambini, F. Giazotto, V. Zannier, L. Sorba, and S. Heun, *Josephson Diode Effect in High-Mobility InSb Nanoflags*, *Nano Lett.* **22**, 8502 (2022).
- [13] M. Trahms, L. Melischek, J. F. Steiner, B. Mahendru, I. Tamir, N. Bogdanoff, O. Peters, G. Reecht, C. B. Winkelmann, F. von Oppen, and K. J. Franke, *Diode effect in Josephson junctions with a single magnetic atom*, *Nature* **615**, 628 (2023).
- [14] W.-S. Du, W. Chen, Y. Zhou, T. Zhou, G. Liu, Z. Zhang, Z. Miao, H. Jia, S. Liu, Y. Zhao, Z. Zhang, T. Chen, N. Wang, W. Huang, Z.-B. Tan, J.-J. Chen, and D.-P. Yu, *Superconducting Diode Effect and Large Magnetochiral Anisotropy in Td-MoTe₂ Thin Film*, arXiv:2303.09052 (2023).
- [15] M. Gupta, G. V. Graziano, M. Pendharkar, J. T. Dong, C. P. Dempsey, C. Palmstrøm, and V. S. Pribiag, *Gate-tunable superconducting diode effect in a three-terminal Josephson device*, *Nat. Commun.* **14**, 3078 (2023).
- [16] A. Gutfreund, H. Matsuki, V. Plastovets, A. Noah, L. Gorzawski, N. Fridman, G. Yang, A. Buzdin, O. Millo, J. W. A. Robinson, and Y. Anahory, *Direct observation of a superconducting vortex diode*, *Nat. Commun.* **14**, 1630 (2023).
- [17] H. Narita, J. Ishizuka, D. Kan, Y. Shimakawa, Y. Yanase, and T. Ono, *Magnetization control of zero-field intrinsic superconducting diode effect*, *Advanced Materials* **35**(40):e2304083 (2023).
- [18] D. Margineda, A. Crippa, E. Strambini, Y. Fukaya, M. T. Mercaldo, M. Cuoco, and F. Giazotto, *Sign reversal diode effect in superconducting Dayem nanobridges*, *Commun. Phys.* **6**, 343 (2023).
- [19] A. Daido, Y. Ikeda, and Y. Yanase, *Intrinsic Superconducting Diode Effect*, *Phys. Rev. Lett.* **128**, 037001 (2022).
- [20] A. Daido and Y. Yanase, *Superconducting diode effect and nonreciprocal transition lines*, *Phys. Rev. B* **106**, 205206 (2022).
- [21] S. Ilić and F. S. Bergeret, *Theory of the Supercurrent Diode Effect in Rashba Superconductors with Arbitrary Disorder*, *Phys. Rev. Lett.* **128**, 177001 (2022).
- [22] N. F. Q. Yuan and L. Fu, *Supercurrent diode effect and finite-momentum superconductors*, *PNAS* **119**, e2119548119 (2022).
- [23] J. J. He, Y. Tanaka, and N. Nagaosa, *A phenomenological theory of superconductor diodes*, *New J. Phys.* **24**, 053014 (2022).
- [24] Y. Zhang, Y. Gu, P. Li, J. Hu, and K. Jiang, *General Theory of Josephson Diodes*, *Phys. Rev. X* **12**, 041013 (2022).
- [25] H. D. Scammell, J. I. A. Li, and M. S. Scheurer, *Theory of zero-field superconducting diode effect in twisted trilayer graphene*, *2D Materials* **9**, 025027 (2022).
- [26] R. S. Souto, M. Leijnse, and C. Schrade, *Josephson Diode Effect in Supercurrent Interferometers*, *Phys. Rev. Lett.* **129**, 267702 (2022).
- [27] H. F. Legg, D. Loss, and J. Klinovaja, *Superconducting diode effect due to magnetochiral anisotropy in topologi-*

- cal insulators and Rashba nanowires*, Phys. Rev. B **106**, 104501 (2022).
- [28] M. Davydova, S. Prembabu, and L. Fu, *Universal Josephson diode effect*, Sci. Adv. **8**, eabo0309 (2022).
- [29] Y. Tanaka, B. Lu, and N. Nagaosa, *Theory of giant diode effect in d-wave superconductor junctions on the surface of a topological insulator*, Phys. Rev. B **106**, 214524 (2022).
- [30] B. Lu, S. Ikegaya, P. Bursset, Y. Tanaka, and N. Nagaosa, *Tunable Josephson Diode Effect on the Surface of Topological Insulators*, Phys. Rev. Lett. **131**, 096001 (2023).
- [31] T. Karabassov, I. V. Bobkova, A. A. Golubov, and A. S. Vasenko, *Hybrid helical state and superconducting diode effect in superconductor ferromagnet/topological insulator heterostructures*, Phys. Rev. B **106**, 224509 (2022).
- [32] J. F. Steiner, L. Melischek, M. Trahms, K. J. Franke, and F. von Oppen, *Diode Effects in Current-Biased Josephson Junctions*, Phys. Rev. Lett. **130**, 177002 (2023).
- [33] D. Kochan, A. Costa, I. Zhumagulov, and I. Žutić, *Phenomenological Theory of the Supercurrent Diode Effect: The Lifshitz Invariant*, arXiv:2303.11975 (2023).
- [34] A. Costa, J. Fabian, and D. Kochan, *Microscopic study of the Josephson supercurrent diode effect in Josephson junctions based on two-dimensional electron gas*, Phys. Rev. B **108**, 054522 (2023).
- [35] J. S. Meyer and M. Houzet, *Josephson diode effect in a ballistic single-channel nanowire*, Appl. Phys. Lett. **125**, 022603 (2024).
- [36] J. Hasan, D. Shaffer, M. Khodas, and A. Levchenko, *Supercurrent diode effect in helical superconductors*, Phys. Rev. B **110**, 024508 (2024).
- [37] H. F. Legg, K. Laubscher, D. Loss, and J. Klinovaja, *Parity protected superconducting diode effect in topological Josephson junctions*, Phys. Rev. B **108**, 214520 (2023).
- [38] J. Cayao, N. Nagaosa, and Y. Tanaka, *Enhancing the Josephson diode effect with Majorana bound states*, Phys. Rev. B **109**, L081405 (2024).
- [39] Z. Liu, L. Huang, and J. Wang, *Josephson Diode Effect in Topological Superconductor*, Phys. Rev. B **110**, 014519 (2024).
- [40] M. Roig, P. Kotetes, and B. M. Andersen, *Superconducting diodes from magnetization gradients*, Phys. Rev. B **109**, 144503 (2024).
- [41] R. Seoane Souto, M. Leijnse, C. Schrade, M. Valentini, G. Katsaros, and J. Danon, *Tuning the Josephson diode response with an ac current*, Phys. Rev. Research **6**, L022002 (2024).
- [42] S. Banerjee and M. S. Scheurer, *Altermagnetic superconducting diode effect*, Phys. Rev. B **110**, 024503 (2024).
- [43] D. Chakraborty and A. M. Black-Schaffer, *Perfect superconducting diode effect in altermagnets*, arXiv:2408.07747 (2024).
- [44] G. L. J. A. Rikken, J. Fölling, P. Wyder, *Electrical Magnetochiral Anisotropy*, Phys. Rev. Lett. **87**, 236602 (2001).
- [45] R. Wakatsuki, Y. Saito, S. Hoshino, Y. M. Itahashi, T. Ideue, M. Ezawa, Y. Iwasa, and N. Nagaosa, *Nonreciprocal charge transport in noncentrosymmetric superconductors*, Sci. Adv. **3**, e1602390 (2017).
- [46] Y. Tokura and N. Nagaosa, *Nonreciprocal responses from non-centrosymmetric quantum materials*, Nat. Commun. **9**, 3740 (2018).
- [47] M. Nadeem, M. S. Fuhrer, and X. Wang, *The superconducting diode effect*, Nat. Rev. Phys. **5**, 558 (2023).
- [48] P. Kotetes, H. O. M. Sura, and B. M. Andersen, *Anatomy of Spin and Current Generation from Magnetization Gradients in Topological Insulators and Rashba Metals*, Phys. Rev. B **108**, 155310 (2023).
- [49] L. Yu, *Bound state in superconductors with paramagnetic impurities*, Acta Phys. Sin. **21**, 75 (1965); H. Shiba, *Classical Spins in Superconductors*, Prog. Theor. Phys. **40**, 435 (1968); A. I. Rusinov, *Theory of gapless superconductivity in alloys containing paramagnetic impurities*, Sov. Phys. JETP **29**, 1101 (1969); A. Sakurai, *Comments on Superconductors with Magnetic Impurities*, Progr. Theor. Phys. **44**, 1472 (1970).
- [50] M. Leijnse and K. Flensberg, *Parity qubits and poor man's Majorana bound states in double quantum dots*, Phys. Rev. B **86**, 134528 (2012).
- [51] A. Tsintzis, R. Seoane Souto, and M. Leijnse, *Creating and detecting poor man's Majorana bound states in interacting quantum dots*, Phys. Rev. B **106**, L201404 (2022).
- [52] A. Tsintzis, R. Seoane Souto, K. Flensberg, J. Danon, and M. Leijnse, *Majorana Qubits and Non-Abelian Physics in Quantum Dot-Based Minimal Kitaev Chains*, PRX Quantum **5**, 010323 (2024).
- [53] R. Seoane Souto and R. Aguado, *Subgap states in semiconductor-superconductor devices for quantum technologies: Andreev qubits and minimal Majorana chains*, arXiv:2404.06592 (2024).
- [54] Y. Tanaka, T. Hirai, K. Kusakabe, and S. Kashiwaya, *Theory of the Josephson effect in a superconductor/one-dimensional electron gas/superconductor junction*, Phys. Rev. B **60**, 6308 (1999).
- [55] K. Sengupta, I. Žutić, H.-J. Kwon, V. M. Yakovenko, and S. Das Sarma, *Midgap Edge States and Pairing Symmetry of Quasi-One-Dimensional Organic Superconductors*, Phys. Rev. B **63**, 144531 (2001).
- [56] A. Y. Kitaev, *Unpaired Majorana Fermions in Quantum Wires*, Phys. Usp. **44**, 131 (2001).
- [57] L. Fu and C. L. Kane, *Josephson Current and Noise at a Superconductor-Quantum Spin Hall Insulator-Superconductor Junction*, Phys. Rev. B **79**, 161408(R) (2009).
- [58] Y. Tanaka, T. Yokoyama, and N. Nagaosa, *Manipulation of the Majorana Fermion, Andreev Reflection, and Josephson Current on Topological Insulators* Phys. Rev. Lett. **103**, 107002 (2009).
- [59] L. Jiang, D. Pekker, J. Alicea, G. Refael, Y. Oreg, and F. von Oppen, *Unconventional Josephson Signatures of Majorana Bound States*, Phys. Rev. Lett. **107**, 236401 (2011).
- [60] P. San-Jose, E. Prada, and R. Aguado, *ac Josephson Effect in Finite-Length Nanowire Junctions with Majorana Modes*, Phys. Rev. Lett. **108**, 257001 (2012).
- [61] P. Kotetes, A. Shnirman, and G. Schön, *Engineering and manipulating topological qubits in 1D quantum wires*, J. Korean Phys. Soc. **62**, 1558 (2013).
- [62] L. Jiang, D. Pekker, J. Alicea, G. Refael, Y. Oreg, A. Brataas, and F. von Oppen, *Magneto-Josephson effects in junctions with Majorana bound states*, Phys. Rev. B **87**, 075438 (2013).
- [63] C. W. J. Beenakker, D. I. Pikulin, T. Hyart, H. Schomeerus, J. P. Dahlhaus, *Fermion-Parity Anomaly of the Critical Supercurrent in the Quantum Spin-Hall Effect*, Phys. Rev. Lett. **110**, 017003 (2013).
- [64] D. Sticlet, C. Bena, and P. Simon, *Josephson Effect in Superconducting Wires Supporting Multiple Majorana*

- Edge States*, Phys. Rev. B **87**, 104509 (2013).
- [65] J. Cayao, A. M. Black-Schaffer, E. Prada, and R. Aguado, *Andreev spectrum and supercurrents in nanowire-based SNS junctions containing Majorana bound states*, Beilstein J. Nanotechnol. **9**, 1339 (2018).
- [66] M. Houzet and J. S. Meyer, *Majorana-Weyl crossings in topological multiterminal junctions* Phys. Rev. B **100**, 014521 (2019).
- [67] H.-Y. Xie and A. Levchenko, *Topological supercurrents interaction and fluctuations in the multiterminal Josephson effect*, Phys. Rev. B **99**, 094519 (2019).
- [68] P. Kotetes, M.-T. Mercaldo, and M. Cuoco, *Synthetic Weyl Points and Chiral Anomaly in Majorana Devices with Nonstandard Andreev-Bound-State Spectra*, Phys. Rev. Lett. **123**, 126802 (2019).
- [69] M.-T. Mercaldo, P. Kotetes, and M. Cuoco, *Magneto-electrically tunable Andreev bound state spectra and spin polarization in p-wave Josephson junctions*, Phys. Rev. B **100**, 104519 (2019).
- [70] K. Sakurai, M.-T. Mercaldo, S. Kobayashi, A. Yamakage, S. Ikegaya, T. Habe, P. Kotetes, M. Cuoco, and Y. Asano, *Nodal Andreev spectra in multi-Majorana three-terminal Josephson junctions*, Phys. Rev. B **101**, 174506 (2020).
- [71] J.-A. Wang, S. Zhou, and P. Kotetes, *Majorana braiding racetracks from charge Chern insulator-superconductor hybrids*, Phys. Rev. B **105**, 045423 (2022).
- [72] M. A. Javed, J. Schwibbert, and R.-P. Riwar, *Fractional Josephson effect versus fractional charge in superconducting-normal metal hybrid circuits*, Phys. Rev. B **107**, 035408 (2023).
- [73] A. V. Balatsky, I. Vekhter, and J.-X. Zhu, *Impurity-induced states in conventional and unconventional superconductors*, Rev. Mod. Phys. **78**, 373 (2006).
- [74] S. Nakosai, Y. Tanaka, and N. Nagaosa, *Two-Dimensional P-Wave Superconducting States with Magnetic Moments on a Conventional S-Wave Superconductor*, Phys. Rev. B **88**, 180503(R) (2013).
- [75] F. Pientka, L. I. Glazman, and F. von Oppen, *Topological Superconducting Phase in Helical Shiba Chains*, Phys. Rev. B **88** 155420 (2013).
- [76] A. Heimes, P. Kotetes, and G. Schön, *Majorana Fermions from Shiba States in an Antiferromagnetic Chain on Top of a Superconductor*, Phys. Rev. B **90**, 060507(R) (2014).
- [77] P. M. R. Brydon, H.-Y. Hui, and J. D. Sau, *Topological Yu-Shiba-Rusinov Chain from Spin-Orbit Coupling*, Phys. Rev. B **91**, 064505 (2015).
- [78] A. Heimes, D. Mendler, and P. Kotetes, *Interplay of Topological Phases in Magnetic Adatom-Chains on Top of a Rashba Superconducting Surface*, New J. Phys. **17**, 023051 (2015).
- [79] S. Ryu, A. Schnyder, A. Furusaki and A. Ludwig, *Topological Insulators and Superconductors: Ten-Fold Way and Dimensional Hierarchy*, New J. Phys. **12**, 065010 (2010).
- [80] S. Nadj-Perge, I. K. Drozdov, Jian Li, Hua Chen, S. Jeon, J. Seo, A. H. MacDonald, B. A. Bernevig, and A. Yazdani, *Observation of Majorana Fermions in Ferromagnetic Atomic Chains on a Superconductor*, Science **346**, 602 (2014).
- [81] S. Jeon, Y. Xie, J. Li, Z. Wang, B. A. Bernevig, and A. Yazdani, *Distinguishing a Majorana Zero Mode Using Spin-Resolved Measurements*, Science **358**, 772 (2017).
- [82] H. Kim, A. Palacio-Morales, T. Posske, L. Rózsa, K. Palotás, L. Szunyogh, M. Thorwart, and R. Wiesendanger, *Toward Tailoring Majorana Bound States in Artificially Constructed Magnetic Atom Chains on Elemental Superconductors*, Science Advances **4**, eaar5251 (2018).
- [83] L. Schneider, S. Brinker, M. Steinbrecher, J. Hermenau, T. Posske, M. dos Santos Dias, S. Lounis, R. Wiesendanger, and J. Wiebe, *Controlling in-gap end states by linking nonmagnetic atoms and artificially-constructed spin chains on superconductors*, Nat. Commun. **11**, 4707 (2020).
- [84] L. Schneider, P. Beck, T. Posske, D. Crawford, E. Mascot, S. Rachel, R. Wiesendanger, and J. Wiebe, *Evidence of topological Shiba bands in artificial spin chains on superconductors*, Nat. Phys. **17**, 943 (2021).
- [85] L. Schneider, P. Beck, L. Rózsa, T. Posske, J. Wiebe, and R. Wiesendanger, *Probing the topologically trivial nature of end states in antiferromagnetic atomic chains on superconductors*, Nat. Commun. **14**, 2742 (2023).
- [86] K. Grove-Rasmussen, G. Steffensen, A. Jellinggaard, M. H. Madsen, R. Žitko, J. Paaske, J. Nygård, *Yu-Shiba-Rusinov screening of spins in double quantum dots*, Nat. Commun. **9**, 2376 (2018).
- [87] J. C. Estrada Saldaña, A. Vekris, G. Steffensen, R. Žitko, P. Krogstrup, J. Paaske, K. Grove-Rasmussen, and J. Nygård, *Supercurrent in a Double Quantum Dot*, Phys. Rev. Lett. **121**, 257701 (2018).
- [88] J. C. Estrada Saldaña, A. Vekris, R. Žitko, G. Steffensen, P. Krogstrup, J. Paaske, K. Grove-Rasmussen, J. Nygård, *Two-Impurity Yu-Shiba-Rusinov States in Coupled Quantum Dots*, Phys. Rev. B **102**, 195143 (2020).
- [89] T. Dvir, G. Wang, N. van Loo, C.-X. Liu, G. P. Mazur, A. Bordin, S. L. D. ten Haaf, J.-Y. Wang, D. van Driel, F. Zatelli, X. Li, F. K. Malinowski, S. Gazibegovic, G. Badawy, E. P. A. M. Bakkers, M. Wimmer, and L. P. Kouwenhoven, *Realization of a minimal Kitaev chain in coupled quantum dots*, Nature **614**, 445 (2023).
- [90] F. Zatelli, D. van Driel, D. Xu, G. Wang, C.-X. Liu, A. Bordin, B. Roovers, G. P. Mazur, N. van Loo, J. Cornelis Wolff, A. M. Bozkurt, G. Badawy, S. Gazibegovic, E. P. A. M. Bakkers, M. Wimmer, L. P. Kouwenhoven, and T. Dvir, *Robust poor man's Majorana zero modes using Yu-Shiba-Rusinov states*, Nat. Commun. **15**, 7933 (2024).
- [91] S. L. D. ten Haaf, Q. Wang, A. M. Bozkurt, C.-X. Liu, I. Kulesh, P. Kim, D. Xiao, C. Thomas, M. J. Manfra, T. Dvir, M. Wimmer, and S. Goswami, *A two-site Kitaev chain in a two-dimensional electron gas*, Nature **630**, 329 (2024).
- [92] J. D. Sau, and S. Das Sarma, *Realizing a robust practical Majorana chain in a quantum-dot-superconductor linear array*, Nat. Commun. **3**, 964 (2012).
- [93] I. C. Fulga, A. Haim, A. R. Akhmerov, and Y. Oreg, *Adaptive tuning of Majorana fermions in a quantum dot chain*, New J. Phys. **15**, 045020 (2013).
- [94] C.-X. Liu, A. M. Bozkurt, F. Zatelli, S. L. D. ten Haaf, T. Dvir, M. Wimmer, *Enhancing the excitation gap of a quantum-dot-based Kitaev chain*, Commun. Phys. **7**, 235 (2024).